International Journal of Material Forming (2021) 14:901–916
https://doi.org/10.1007/s12289-020-01603-7

ORIGINAL RESEARCH

Development of a numerical compensation framework for geometrical deviations in bulk metal forming exploiting a surrogate model and computed compatible stresses

Lorenzo Scandola[1] · Christoph Büdenbender[2] · Michael Till[2] · Daniel Maier[1] · Michael Ott[1] · Bernd-Arno Behrens[2] · Wolfram Volk[1]

Received: 21 April 2020 / Accepted: 22 November 2020 / Published online: 26 February 2021

Abstract

The optimal design of the tools in bulk metal forming is a crucial task in the early design phase and greatly affects the final accuracy of the parts. The process of tool geometry assessment is resource- and time-consuming, as it consists of experience-based procedures. In this paper, a compensation method is developed with the aim to reduce geometrical deviations in hot forged parts. In order to simplify the transition process between the discrete finite-element (FE) mesh and the computer-aided-design (CAD) geometry, a strategy featuring an equivalent surrogate model is proposed. The deviations are evaluated on a reduced set of reference points on the nominal geometry and transferred to the FE nodes. The compensation approach represents a modification of the displacement-compatible spring-forward method (DC-SF), which consists of two elastic FE analyses. The compatible stress originating the deviations is estimated and subsequently applied to the original nominal geometry. After stress relaxation, an updated nominal geometry of the part is obtained, whose surfaces represent the compensated tools. The compensation method is verified by means of finite element simulations and the robustness of the algorithm is demonstrated with an additional test geometry. Finally, the compensation strategy is validated experimentally.

Keywords Compensation · Geometrical deviations · Bulk metal forming · Surrogate model · Tool design · Compatible stresses

Introduction

The design of tools used in hot forging processes represents a fundamental step in the product development of hot-forged components [1]. The extremely critical environment required for hot forming is responsible for an inhomogeneous temperature distribution accompanied by complex residual tension fields. These factors result in geometrical deviations from the nominal geometry [2]. Since predicting such behaviour with a physically-based approach would necessitate material models that are frequently unavailable [3], deviation compensation is generally performed by direct geometrical tuning of the forming tools. Although it is common practice in the industry to adapt tool geometry on an *experience-driven* basis, this results in considerable costs and time overruns. Conversely, it is crucial to dispose of an efficient *data-driven* strategy for tool geometry assessment in the early design phase, since the dimensional accuracy of the products must be ensured and guaranteed for the whole lifetime of the tools [4]. To this extent, the combination of the forming simulation with a virtual compensation strategy can be successfully employed to simplify the iterative process that leads to optimal tool geometry. Nevertheless, the transition between the continuous CAD environment and the discrete FE mesh remains a considerable issue. To enable manufacture, the final updated tool geometry must be delivered in a parametric format, such as .stp or .igs files. On the other hand, the deviating geometry is obtained either by forming simulation results or by point clouds acquired experimentally through optical metrology systems, which are represented by triangulated meshes, like .stl files. A robust approach is required to efficiently retrieve

✉ Lorenzo Scandola
lorenzo.scandola@utg.de

[1] Chair of Metal Forming and Casting, Technical University of Munich, Walther-Meißner-Straße 4, 85748 Garching b. München, Germany

[2] Institute of Forming Technology and Machines, Leibniz Universität Hannover, An der Universität 2, 30823 Garbsen, Germany

the parametrically compensated data from the discrete simulation results. The aim of this job is to propose an efficient framework for geometrical compensation of rotational symmetric bulk formed parts. This is obtained by developing an equivalent surrogate model based on reference points. Moreover, the stress-based compensation strategy of the Displacement-Compatible Spring-Forward method (DC-SF) originally presented by Lee [5] is modified and enhanced. Finally, the developed strategy is verified by two numerical examples, and its suitability to tackle industrial problems is demonstrated.

State of the art

In order to perform the geometrical compensation in hot forming, it is fundamental to distinguish the origin of the deviations under investigation, Fig. 1a. As described by Hartmann [6], stochastic deviations are typically related to a variation in the current operating conditions, such as tribological interactions, material properties fluctuations and temperature oscillations. Such sources of deviation can hardly be identified and can only be tackled through real-time parameter adjustment techniques. On the other hand, deterministic factors can derive from inherent errors in the employed model or from simplified assumptions in the process design, and are characterised by a marked repeatability. These are the only deviation sources that a geometrical compensation model can identify and account for. After successful compensation, the parts are still affected by deviations of stochastic nature, which cause an oscillation in the solution around a design point and set the need for stopping criteria.

Tool geometry modification techniques are particularly established in sheet metal forming. Shape inaccuracy in this field is mainly due to elastic springback, which is typically challenging to simulate [7] and linked to high measuring effort [8]. Karafillis and Boyce [9] developed the spring-forward method (SF) [10], which comprises an inverse simulation of the springback through application of the internal forces [11]. An evolution of such a method was suggested by Wu [12], who proposed an iterative algorithm with mesh generation options [13]. The geometrically-based Displacement-Adjustment method (DA) was established by Gan and Wagoner [14] and consists in displacing the deviating nodes by the exact amount of the calculated deviations. The superior convergence behaviour of such technique has been proved by Lingbeeck [15], while Birkert [16] investigated the impact of the compensation direction. The definition of the springback driving stress as the difference between residual and forming stresses is the core of the springback cause analysis method by Hiramoto [17]. Some preliminary investigations involving sheet metal tests have been performed by Lee [5], who proposed the Displacement-Compatible Spring-Forward (DC-SF) method. This strategy involves a two-step process. First, the current geometry, $CURR$, is deformed to the nominal one, TGT, by applying the inverted deviation field, $-u$, as a nodal displacement boundary conditions field. This generates in the $CURR$ part a displacement compatible stress field, σ_{dc}, which is responsible for the arising of deviations. In the second step, this stress field is inverted and relaxation occurs. The shape obtained through this step from the original nominal geometry represents the updated nominal geometry, which minimises the deviations.

In hot forming of bulk components complex thermomechanical interactions and additional phenomena arise, such as the elastic deformation of the tools and the volumetric shrinkage of the parts after cooling [2]. Fourment [18] suggested a shape optimisation method for a two-step forging process, while Vieilledent focused on the optimisation

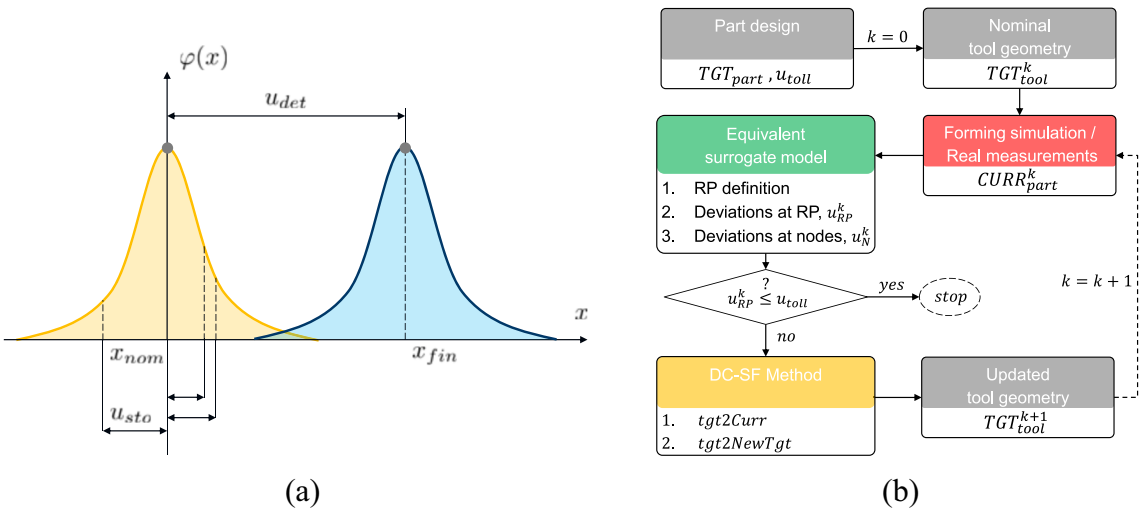

Fig. 1 **a** Deterministic and stochastic deviations; **b** Iterative compensation process

of the preform geometry using B-Splines [19]. The implementation of a shell for coupling FE analysis and shape die optimisation is described in the work of Rodič [20]. In a further contribution Ghouati and Gelin propose the optimal design of forming processes exploiting a seqential quadratic programming approach [21]. In the work of Ou [22] the importance of die elasticity and thermal distorsion is highlighted and the compensation is attained through weighting factors. Lu [23] investigated airfoil blades obtained by net-shape forging and employed B-spline surface approximation. Landkammer developed an inverse form finding method [24] and employed a shape optimisation approach[25], while Caspari [26] focused on node recognition strategies between different configurations. A fully geometry-based compensation rule was developed by Hartmann and Eder [27], who succeeded in performing the compensation on a set of user-defined surface points through shape morphing of the nominal geometry [28]. The material point tracking method (MPT) was proposed in the work of Maier [4]. By mapping the tool and part geometry by means of the so-called material points, a deviation-dependent compensation direction can be defined, in contrast to the typical normal or forming directions approaches.

Problem definition and iterative compensation problem

The problem of the compensation of geometrical deviations by adapting the tool geometry is an iterative process, which is illustrated in Fig. 1b. The aim of the procedure is to achieve a final geometry of the part, TGT_{part}, which lies bet ween the tolerances defined in the design step, u_{toll}. From the nominal geometry of the part, the first tool geometry is derived, TGT^{k}_{tool}. The forming simulation or the conduction of real tests provide the data for the current geometry of the part, $CURR^{k}_{part}$. At this point, the equivalent surrogate model is employed. The reference points are defined and their deviations assessed, u^{k}_{RP}. If they exceed the permitted tolerances, the DC-SF method is employed and an updated tool geometry is derived, TGT^{k+1}_{tool}. In the next iteration, the impact of the updated tools is evaluated by assessing the deviations of the new part. The process ends once the required part accuracy has been achieved. In the following, the developed compensation framework is presented, describing the features of the surrogate model and the principles of the enhanced DC-SF compensation algorithm.

Generation of the equivalent surrogate model

The most critical aspect when performing a geometrical tool compensation is represented by the different nature of the required input data. While the nominal CAD files are usually expressed in parametric form, which is supported by analytic curves or surfaces, the current data from simulation or measurements are a collection of facets and vertices. In the case of 3D-scanning experimental measurements, the density of the cloud depends on the applied resolution, while for FE analyses the approximation of the discretised geometry is related to the mesh shape and refinement [29]. Since the compensation workflow requires a continuous comparison between parametric and triangulated files in order to assess deviations and extract the compensated final shape, it is advantageous to employ an equivalent reference points-based surrogate model. By substituting the nominal parametrised geometry under investigation with the reference points-based surrogate model, a smooth transition

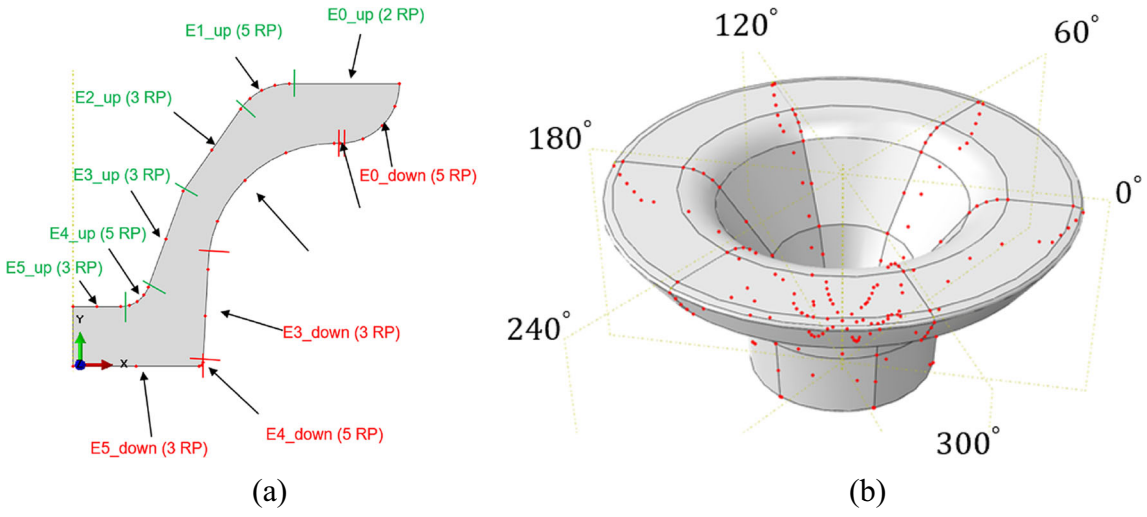

(a) (b)

Fig. 2 Case-study geometry: **a** cross-section partitioning; **b** radial partitioning

Table 1 Reference points definition criteria

	Minimum	Maximum
Lines	2 RP	3 RP
Arcs	3 RP	5 RP

between the discrete FE and continuous CAD world can be obtained. The deviations are only calculated at the reference points and then extrapolated at the other nodes by interpolation. The accuracy of the surrogate model largely depends on the choice of the reference points. Criteria must be defined to ensure the relevance of the chosen points for interpolating the tool geometry. In the following, the processes of selecting the reference points, assessing their deviations and extrapolating the nodal deviation field are discussed.

Reference points determination

The strategy for the definition of the reference points is presented for the case-study of a rotational symmetrical hot-forged component, which exhibits pronounced deviations. The reference points are obtained through a two-step partitioning procedure, which is carried out in Abaqus^{TM} [30] through automated Python^{TM} scripts [31]. First of all, a *cross-sectional partitioning* is carried out, as shown in Fig. 2a. The generic cross-section contour of the part is subdivided into a suitable number of segments allowing to describe its geometrical features, to which a variable number of equidistant reference points are associated. The basic criterion to assess the number of reference points per segment is the evaluation of the capability of such a set of points of representing the associated geometrical contour by B-splines interpolation. Although some general rules can be defined on the basis of the shape and length of the segments, Table 1, this is a highly user-dependent task. For the investigated geometry, 8 segments are selected in the upper contour and 8 in the lower contour, and the reference points for each segment are accordingly identified, resulting in a total number of 38 points. Successively, a *radial partitioning* is carried out. An angular range is set by the user and the cross-sectional reference points are repeated on any resulting cross-section, Fig. 2b. As the choice of the angular range is arbitrary and depends on the user, a sensitivity investigation is performed. Increasing the number of cross-sections results in a more precise deviations assessment but increases the computational cost. To identify a suitable number of radial partitions, the reference points from each partition are superimposed onto a single cross-section and the mean deviation is calculated. The tests performed with 6, 36 and 360 partitions show a mean deviation of below 0.5%, Fig. 3. For this reason, 6 partitions are identified as the most efficient solution, which corresponds to an angular range of 60° degrees and to a total number of 228 reference points. The developed surrogate

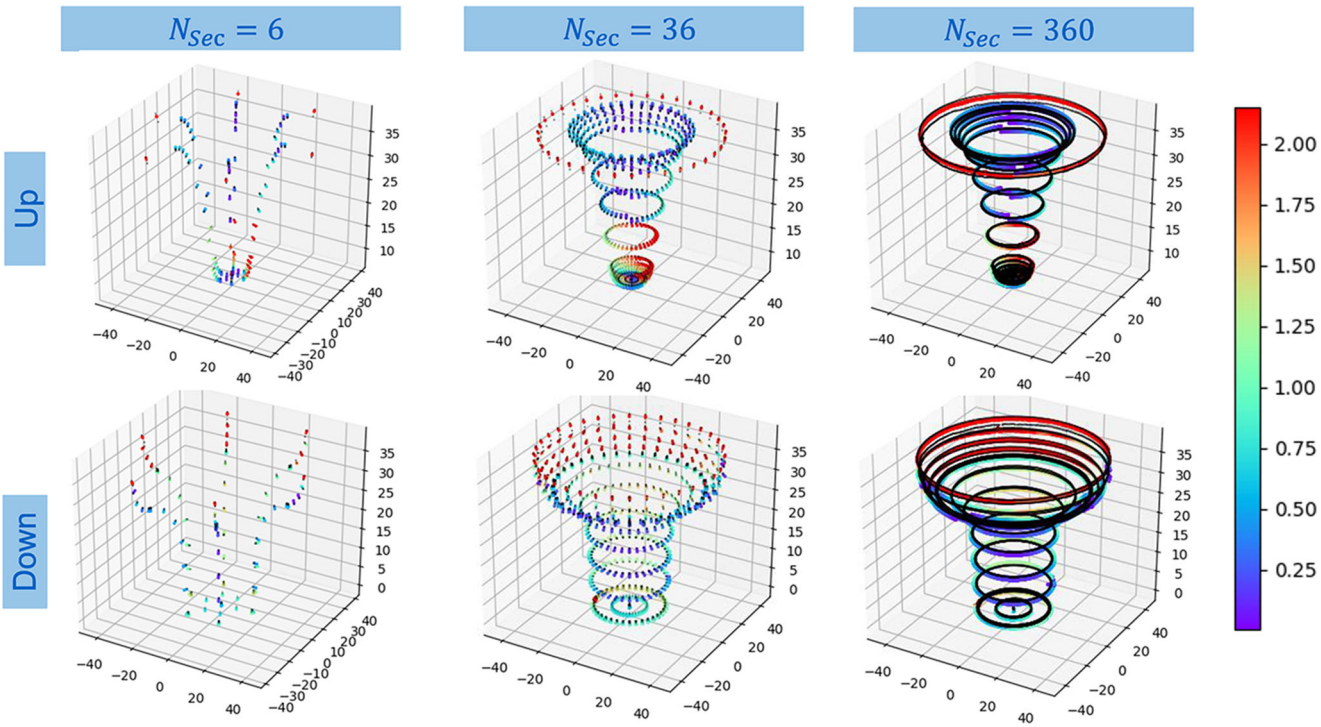

Fig. 3 Sensitivity analysis on reference points number

model is able to generate relevant reference points for 3D-rotational symmetrical as well as for 2D-cross-sections and can be used both with real measurements and simulation results.

Deviation assessment

As the part under investigation exhibits rotational symmetry, the compensation process can be carried out with 2D-axisymmetric analyses. The deviations of the reference points must be assessed on a single cross-section, where the nodal deviations can be extrapolated. Depending on the input data representing the final deviating geometry, two different strategies are available. In the case of 3D-scanning data, a closest-neighbours approach making use of a k-D-trees algorithm is employed. The results are then superimposed onto a cross-section and averaged, as shown in Figs. 4a, b, and c. The aim of such approach is to minimise the impact of stochastic effects, which cannot be handled in the compensation strategy. These include anisotropic flow during forming, which is not captured by the adopted isotropic material models, as well as the presence of craters or oxide layers on the measured parts. In addition, eccentricity errors due to the imprecise manual positioning of the parts in the tools are successfully mitigated. For axisymmetric forming simulation results, Figs. 4d and e, the deviations are estimated by computing the normal distance between the reference point and the line generated by its closest experimental points, $u^{\perp}$ in Fig. 4f. This enables a more robust approximation of the deviation compared to the distance between the reference point and anyone of its closest points, u_{i-1}, u_i and u_{i+1}. Regardless of the origin, whether simulated or measured, and the type, 3D or 2D, of the data representing the produced geometry, this approach allows the efficient assignment of the deviation values to the user-defined reference points. This is the benefit of the surrogate model, which can be exploited to retrieve the data for the compensation finite element model.

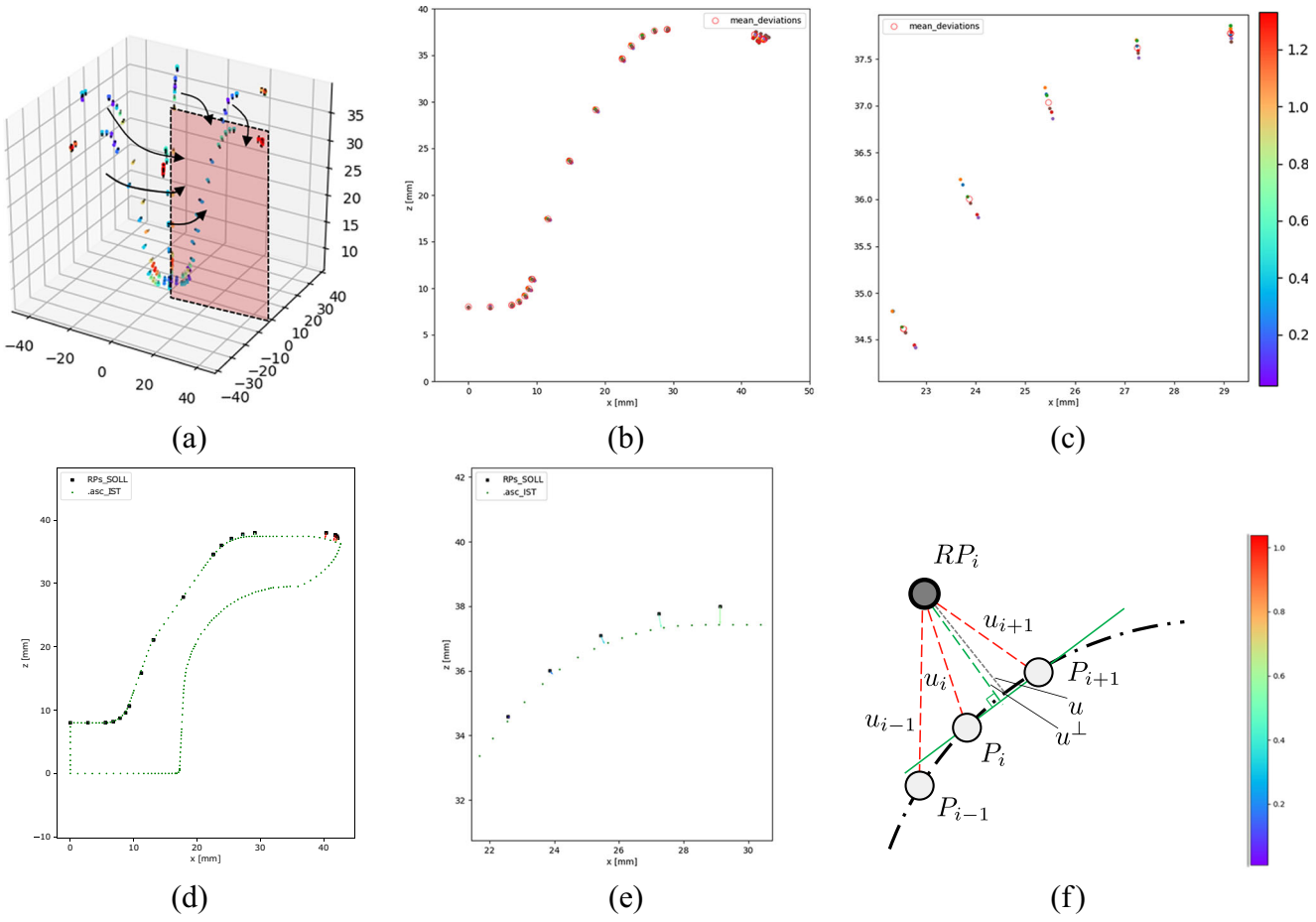

Fig. 4 Reference points deviations assessment from 3D measurements (above) and 2D axisymmetric forming simulations (below): **a** Closest-neighbours deviation assessment from 3D-measurements; **b** averaging of reference points deviations; **c** detail of the superimposed deviating reference points; **d** normal distance deviation assessment from 2D-simulations; **e** detail of the normal deviation assessment in the radius; **f** principle of deviation assessment of a reference point, RP_i, from its closest measurement points, P_{i-1}, P_i, P_{i+1} on the current geometry (dash-dot line)

Nodal deviation extrapolation

Once the deviations at the reference points are available, the contour of the deviating geometry is interpolated through B-splines. B-splines curves are piecewise polynomial non-rational functions defined as [32]:

$$\mathbf{C}(u) = \sum_{i=0}^{n} N_{i,p}(u)\mathbf{P}_i, \qquad 0 = a \leq u \leq 1 \tag{1}$$

where p is the degree, $\mathbf{P}_i$ represent the control points, $N_{i,p}(u)$ are the B-spline basis functions and $U = \{a, \ldots, b\}$ is the knot vector containing the m knots, which are linked by the fundamental relation:

$$m = n + p + 1 \tag{2}$$

Thanks to the property of the local support they are particularly suitable for representing local geometrical details. In addition, they can be turned to NURBS, of which they represent a particular case. The deviated reference points are fed as input to the centripetal interpolation algorithm available in the package NURBSpython [33], which returns the best fitting B-splines. This allows obtaining a parametric continuous description, from which the nodal deviations can be extrapolated. Independently on the density of the mesh, the displacement boundary conditions field can be retrieved with the normal distance methods, as shown in Figs. 5a and b.

The enhanced DC-SF: a stress-based compensation method

The strategy adopted to perform the compensation is an enhancement of the Displacement-Compatible Spring-Forward method by Lee [5]. The original technique prescribes to deform the obtained deviating geometry, $CURR$, back to the nominal shape, TGT, in order to reproduce the compatible stress field. Subsequently, the recorded stress field is relaxed and the updated shape is obtained. While this procedure is straight-forward, some issues arise in the first step, regarding the application of the deviation field to the FE model of the obtained geometry. The data representing the obtained geometry are in fact either digital measurements of an actually produced prototype or the results of a forming simulation, typically obtained with a different mesh and model to those of the forming simulation. It is therefore necessary to carry out a preliminary surface reconstruction to dispose of the parametric model of the $CURR$ part, which results in a lengthy, cumbersome and imprecise process. Furthermore, the inversion of the displacement compatible stress field in the second step is not a trivial task, as it involves changing the sign of every stress component at every integration point. The approach developed in the enhanced DC-SF method aims to overcome these limitations, resulting in a slightly modified procedure, Fig. 6. The only required parametric model is that of the TGT geometry, which is available from the beginning of the design process. In the first step, *tgt2Curr*, the TGT

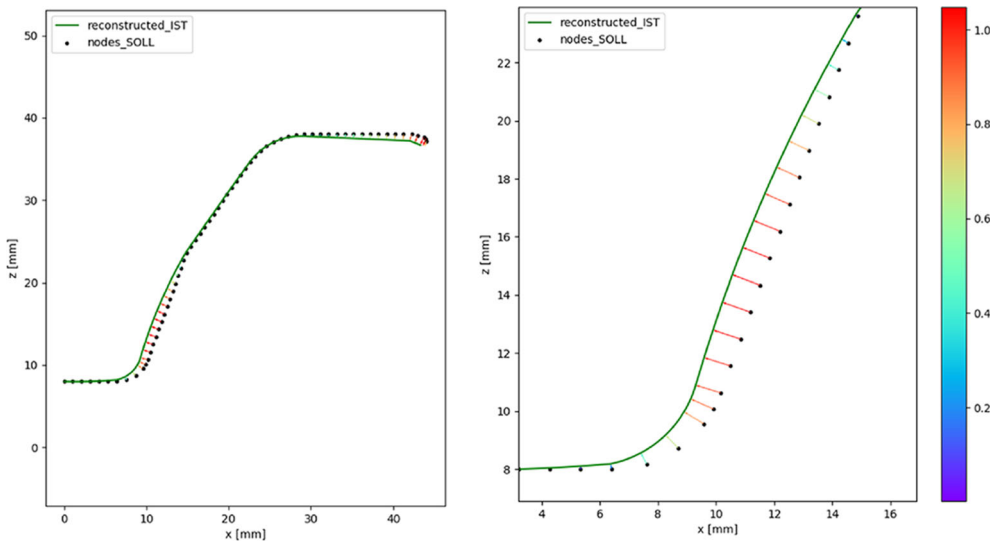

(a) (b)

Fig. 5 Nodal deviations extrapolation: **a** upper contour overview; **b** upper contour detail

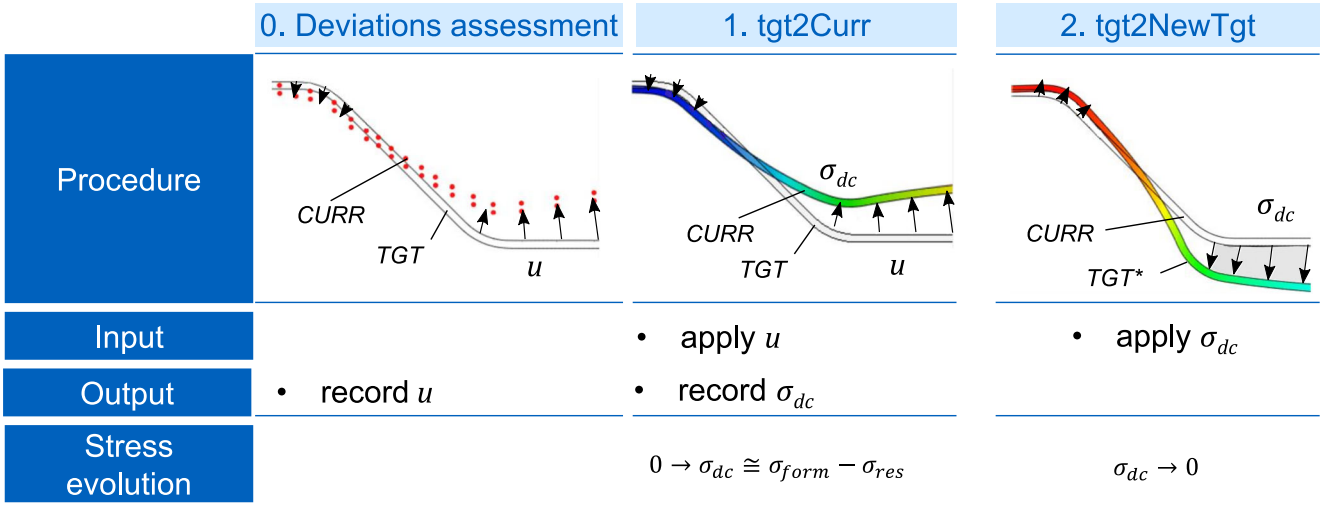

Fig. 6 Theoretical background of the enhanced DC-SF method

part is deformed to the $CURR$ part by applying the deviation field retrieved with the surrogate model, Fig. 7a. This step is carried out as an elastic analysis and only linear elastic material properties are considered, under the hypothesis of compatible displacement. In addition, this means that eventual thermal effects deriving from a hot-forming process are directly included in the shape of the current part, and no thermally-coupled simulation are to be carried out. For this reason, thermal expansion coefficients do not constitute an input of the simulations and do not have any direct influence on the compensation algorithm. In contrast to the resulting residual stress field deriving from a proper forming simulation, in which material non-linearities, contact, tribology and plasticity are taken into account, the stress field arising in this step represents that fraction of the residual stress which is responsible for the deviation, namely the compatible stress field σ_{dc}.

In this way, it is not necessary to retrieve the $CURR$ parametric model from the measurement data. As in the original DC-SF, the second step, *tgt2NewTgt*, consists of the application and relaxation of the displacement compatible stress field, Fig. 7b. In the modified method, the sign of the extracted stress field is already correct and does not require inversion. In addition, the stress components for each integration point are applied as initial conditions on the nominal geometry. Since the only model employed is the parametric model of the nominal geometry, the simulation model of the first and second steps can consist of the same FE mesh, which represents a great advantage when defining the boundary conditions. The simulations are performed with a static step in Abaqus/Standard™ and automated with Python™ scripts. The model consists of 652 nodes and 577 axisymmetric 4-node bilinear quadrilateral elements CAX4R, which allow the reduction

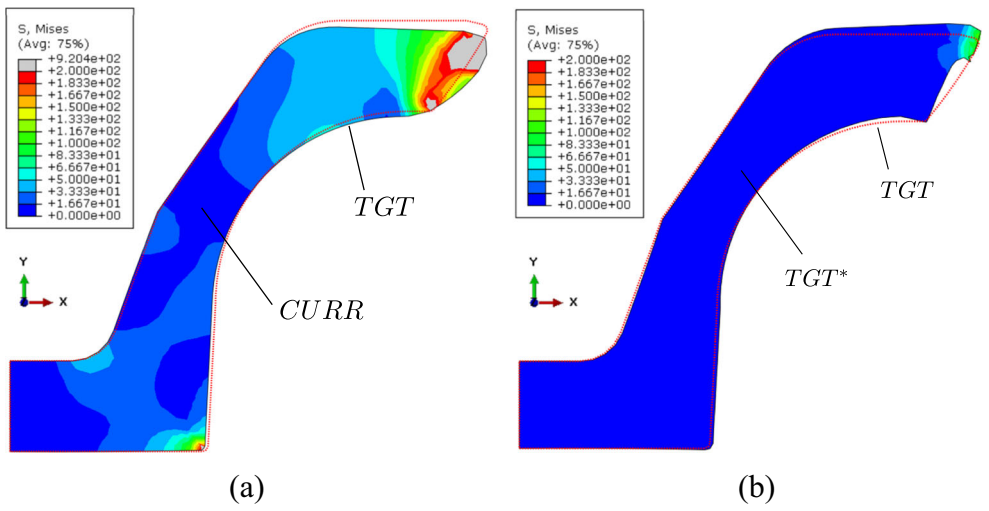

Fig. 7 Von Mises stress in the **a** *tgt2Curr* and **b** *tgt2newTgt* steps

of the problem to two dimensions by exploiting cylindrical coordinates. Furthermore, reduced integration and hourglass control are employed. The boundary conditions in the *tgt2Curr* simulation are the extracted nodal deviations applied as displacement boundary conditions, while the compatible stress field in *tgt2NewTgt* are loaded as initial conditions with the user subroutine SIGINI. The subroutine applies previously extracted stress values to the integration and section points of every element, thus enabling the transfer of compatible stresses between the deformed and undeformed configurations, by identifying same elements through their labels. As for the elastic material properties, the Poisson ratio is set to 0.3, while the Young's modulus represents a scale factor. Since the displacement and hence the deformation field are given, the values of the generated stress field depend in magnitude on the stiffness tensor, whereas their pointing directions are obtained independently through relaxation. This underlines the physically-based nature of the DC-SF method, which automatically retrieves the correct compensation direction for each node, removing the additional degree of freedom of the displacement-based methods represented by the arbitrary choice of the compensation direction.

Tools' reconstruction

To perform the tools' reconstruction the following approach is presented. First of all, it is necessary to derive CAD suitable data from the simulation results. Moreover, the updated geometries of the tools must be extracted from that of the part, ensuring that no modifications to the process configuration are required. In order to obtain a parametric description of the updated part geometry obtained in the simulation, the updated position of the reference points is extracted and interpolated again with B-splines. This allows to ease the transition from triangulated FE compensation results to CAD suitable data, by making use of the equivalent surrogate model only. Under the hypothesis that at the point of maximum loading the tools and the part are fully in contact, the upper and lower contours of the nominal geometry can be identified as effective contours, i.e. they simultaneously represent the updated shape of the part as well that of the tools. The final geometry of the tools can be finally derived by substituting the nominal effective contours with the updated one in a conventional CAD programme, such as Catia V5 [34]. By rotating the determined geometries, the parts required for tool manufacturing are obtained as rotational volume bodies, as shown in Fig. 8. As a remark, since the case study under investigation involves open-die hot-forging, the flange contour is excluded. Although in open-die forging the flange geometry cannot be defined a-priori, the user is required to propose a target geometry for the flange region as well. Depending on the user's choice, this may lead to an unrealistic mismatch between the target and current geometries, which cannot be ascribed to geometrical deviations. This is the case for the deformed shape in Figs. 7a and b, which is not relevant for the purpose of compensation and is therefore neglected.

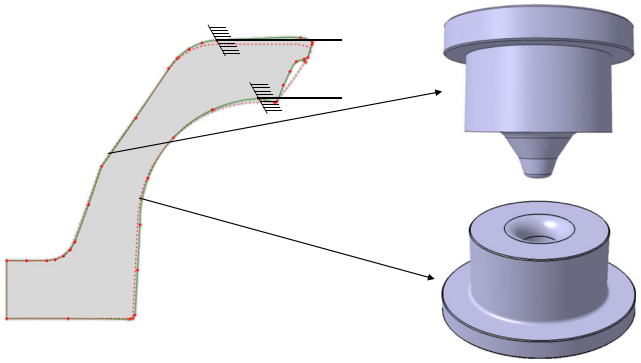

Fig. 8 Design of the tools from the compensated effective contours of the part

Compensation results and method verification

The results of the virtual compensation process for the investigated case study are shown in Figs. 9a and b. As input data for the obtained geometry, $CURR^{k}_{part}$ in Fig. 1b, simulation results from the software Simufact Forging [35] are employed. In order to evaluate the outcome of the compensation, different scalar criteria representative of the deviations of the entire part are employed. The average deviation's magnitude of the reference points for the iteration k, $\bar{u}^k$, is defined as:

$$\bar{u}^k = \sum_{i=n^{RP}_{start}}^{n^{RP}_{end}} \frac{\sqrt{{u^i_x}^2 + {u^i_y}^2 + {u^i_z}^2}}{n^{tot}_{RP}}\Big|_k = \sum_{i=n^{RP}_{start}}^{n^{RP}_{end}} \frac{u^k_{mag}}{n^{tot}_{RP}} \tag{3}$$

and allows to evaluate the achieved tolerance class. In order to assess the performance of the compensation between the iterations, the relative and absolute deviation variations are defined respectively as $\Delta u\%^k_{rel}$ and $\Delta u\%^k_{abs}$:

$$\Delta u\%^k_{rel} = \frac{\bar{u}^{k+1} - \bar{u}^k}{\bar{u}^k} \cdot 100, \qquad \Delta u\%^k_{abs} = \frac{\bar{u}^k - \bar{u}^0}{\bar{u}^0} \cdot 100 \tag{4}$$

The above-mentioned indicators are employed to evaluate the convergence process by performing a manual reading of the results at every iteration. The optimum is achieved

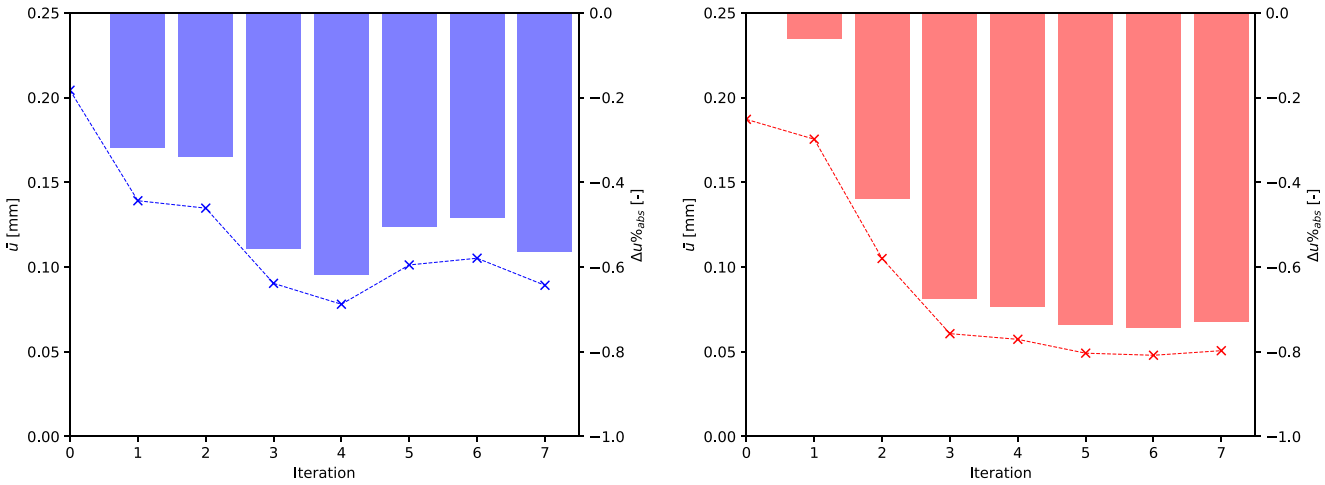

Fig. 9 Average deviation $\bar{u}$ and absolute deviation variation $\Delta u\%_{abs}$: **a** case-study geometry, upper contour; **b** case-study geometry, lower contour

when the average deviation is lower than the target tolerance class value, or when the relative deviation variation does not improve significantly in the next two iterations. In the evaluation of $\bar{u}^k$, the reference points in the flange area are not considered, since they do not contribute to the tool generation. They correspond to the segments labelled 0, 1 and 0, 1, 2 in the upper and lower contours respectively, as shown in Fig. 2a. Although it can be observed that the part accuracy is already significantly enhanced after two iterations, a total number of 7 iterations is carried out to investigate the convergence behaviour of the algorithm and to examine its efficiency. After the fourth iteration, the average deviation in the lower tool exhibits asymptotic behaviour towards 0.05 mm, while the upper one begins oscillating at around 0.08 mm. This suggests that the limits of the process have been reached for the part under investigation and no further reduction in deviation is possible, due to process instabilities. For this reason, the tools deriving from this iteration are identified as the optimal solution, corresponding to absolute deviation variations of -61.8% and -69.4% in the upper and lower tool respectively. This makes it possible to attain an accuracy of the tolerance class $IT8 \div 10$, such as is typical of precision forging [36].

In order to demonstrate the robustness of the compensation method, an additional nominal geometry is investigated. This is shown in Fig. 10a and is constituted of 31 reference points on the cross-section, Fig. 10b. Due to the smoother features of the new geometry, the compensation converges more quickly and the optimal solution is identified in the second iteration, as depicted in Figs. 11a and b. This results in an average deviation of 0.03 mm for both the upper and lower tools and to absolute deviation variations of -80.2% and -82.9% respectively, which again corresponds to the tolerance class $IT8$. The two presented case-studies demonstrate the verification of the method and its ability to reduce deviations on the basis of simulated results.

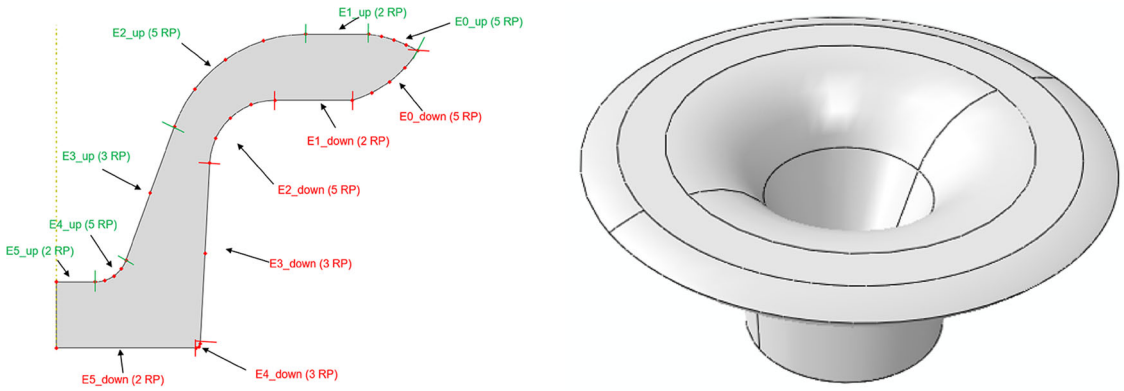

Fig. 10 Robustness analysis geometry: **a** cross-section partitioning; **b** nominal part geometry

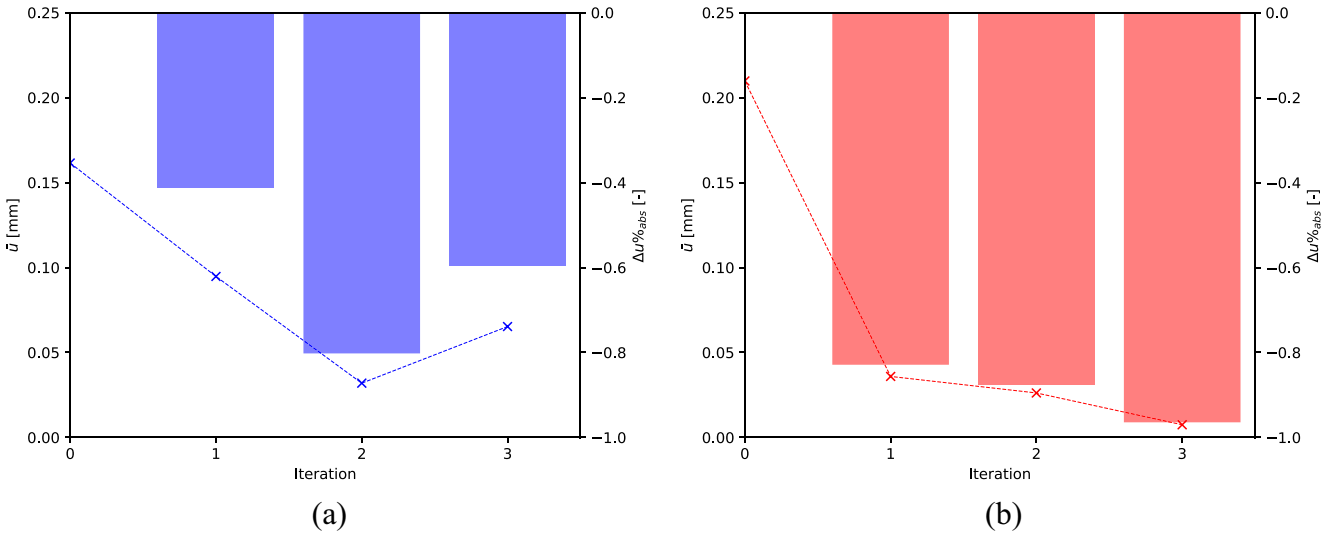

Fig. 11 Average deviation $\bar{u}$ and absolute deviation variation $\Delta u\%_{abs}$: **a** robust-study geometry, upper contour; **b** robust-study geometry, lower contour

Validation and comparison of simulations and experimental results

After successful verification of the compensation algorithm, the method is validated by conducting real tests and analysing experimental data [35]. The forging operations are carried out on a mechanical screw press "Lasco - SPR 500" in open-die forging configuration, the burr originating from the flange zone. The tool material is the steel 1.2714 (55NiCrMoV7), while the part material is the grade 1.7225 (42CrMo4). The forming temperature is 1250°C and the tools are subjected to a pre-heating stage to achieve a starting temperature of 250°C. An homogeneous temperature distribution in the billets is obtained by heating them for 15 minutes in a chamber furnace. Additional information about the performed tests and the forming simulations are available in [35]. The initial tools are produced from the effective contours of the nominal part. The compensated tools are manufactured from the design resulting from the fourth iteration of the virtual compensation, shown in Figs. 9a and b, which in the virtual compensation is chosen as the optimal solution. A series of three specimens is produced with both the initial and the compensated tools. The process parameters are given in Table 2. The components are finally cooled in air and measured with the system "GOM-Atos II 400". In this way, 3D-triangulated surface data required for the assessment of the deviations through the surrogate model are obtained.

The results are shown in Figs. 12a, b, c and d. It can be observed, that both in the upper and lower contours of the nominal geometry the deviations could significantly be reduced also in the manufactured parts obtained with the prototyped tools. A first remark concerns the initial deviations values in the virtually reproduced process and the experimental results. As shown in Figs. 12a and b, the average deviation related to the nominal tools is around 0.2 mm for both contours of the simulated data, while higher values are observed in the manufactured parts, around 0.3 mm and 0.5 mm for the upper and lower contour respectively. This can be also considered the reason for the higher disparity between the experimental results and the simulations in the lower contour, which differ before compensation (iteration 0) by a factor of 3. Nevertheless, an enhancement from $IT13$, typical for open-die forging [36], to $IT10$ in the upper contour and from $IT14$ to $IT13$ in the lower one can be observed. In addition, a high scatter in the experimental data is observed. This is due to the stochastic part of the deviation, which as described above, cannot be treated in the presented framework and would require an enhanced compensation strategy with an inline monitoring and controlling system. Furthermore, it can be noted that the minimum deviations values from the fourth iteration (continuous blue line) cannot be achieved experimentally. This is also expected and highlights the still marked impact of stochastic fluctuations, despite the averaging process used in the assessment procedure of the

Table 2 Process parameter for the experimental open-die forging [35]

Tool material	Part material	Forming temperature	Tool temperature
1.2714 (55NiCrMoV7)	1.7225 (42CrMo4)	1250°C	250°C

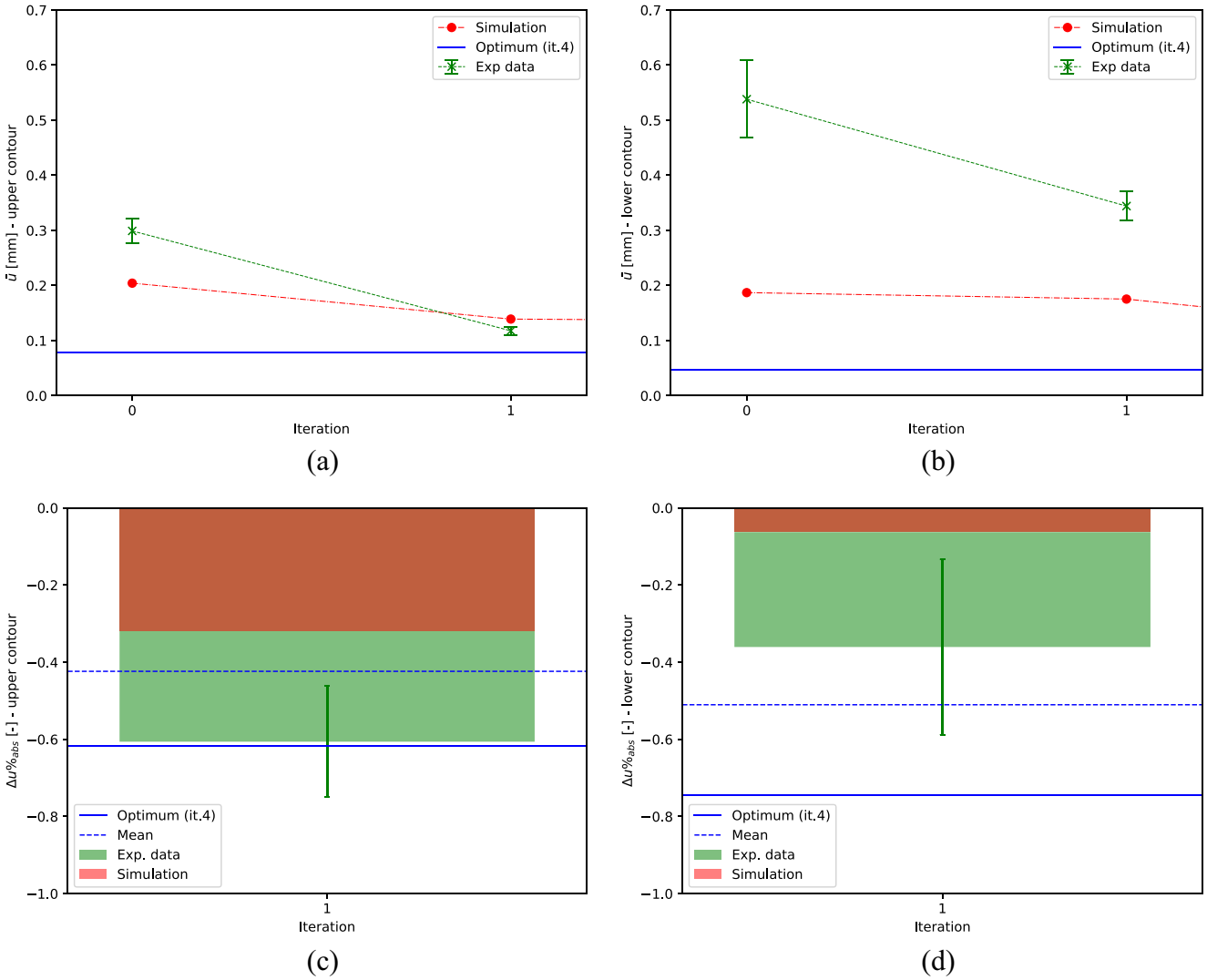

Fig. 12 Comparison of simulation and experimental results: **a** Average deviation $\bar{u}$, upper contour; **b** Average deviation $\bar{u}$, lower contour. **c** Absolute deviation variation $\Delta u\%_{abs}$, upper contour; **d** Absolute deviation variation $\Delta u\%_{abs}$, lower contour

reference points. Nevertheless, the trend of the deviation agrees with the simulated results, as can be seen by comparing the experimental and virtual data of the first iteration. In the case of the upper contour, Fig. 12c, the reduction of deviations is more pronounced than predicted and an absolute deviation variation of up to -60.6% is achieved, in contrast to the -31.9% of the simulation. Also in the lower contour, Fig. 12d, a more effective reduction is obtained and absolute variations of -36.1% are recorded against the predicted -6.3%, although the average deviation values are significantly higher, at about 0.34 mm for the prototype and 0.18 mm for the simulation. Moreover, it can be appreciated that the mean values of the absolute deviation variation from the simulations match or are extremely close to the experimental ones, considering their uncertainty of up to 20%, Fig. 12c and d. This is an additional proof of the validation of the method, while the observed scatter can be taken as representative of the degree of reproducibility of the process. The developed compensation framework is successful in significantly reducing the deterministic part of the geometrical deviation arising in hot open-die forging a nd its capability to handle industrial components is demonstrated.

Discussion

The developed compensation framework allows to ease the process of tools assessment for hot bulk metal forming.

The employment of the equivalent surrogate model enhances the efficiency of the iterative compensation process. Both the deviating contour of the part and the updated shape of the tools are derived from the deviations of a relatively small set of reference points, whose definitions

rely only on the nominal geometry of the part. On the one hand, this reduces the effort needed to measure the deviations, which can be obtained with both 3D-scanning techniques and tactile instruments. Nevertheless, the choice of the reference points has a crucial impact on the accuracy of the predictions and is a highly user-dependent task.

The updated position of the reference points, from which the compensated tools are derived, is obtained with the enhanced DC-SF method. In contrast to the original strategy, where deviations are inverted in sign and the final geometry is deformed to the nominal one, the stress field arising in the *tgt2Curr* step of the enhanced DC-SF represents the physically compatible stress with the correct sign. Since the final geometry, $CURR^{k}_{part}$, is the result of forming simulations or performed tests, the compatibility condition is always verified between the nominal and final geometry in this compensation step, whose aim is to reproduce virtually the shrinkage on the basis of geometrical considerations only. Moreover, the obtained compatible stress field, represents the fraction of the broader residual stress field that directly causes deviations in the part. Since the deformation of the nominal geometry to the final one by application of the deviations field is done on a stress-free nominal geometry, the stress state of the deformed geometry will exhibit only compatible stresses, instead of the forming residual stresses that would arise in the forming simulation or in the real process. This peculiarity makes it possible to dispose of a physical stress-based deviation direction for every node, which represents a clear advantage with respect to the approaches of the normal of forming direction. In addition, the hypothesis of compatible displacements permits to take into consideration the elastic behaviour of the material only, without a complex consideration of plasticity in the compensation simulation. This ensures reduced computational times and a good convergence behaviour. Finally, it should be emphasised that only the nominal geometry of the part is required for the purpose of compensation simulation. Complex non-linear phenomena typical of hot-forging simulations, such as friction, inhomogeneous temperature distribution, contact and elasto-plastic behaviour of the tools are implicitly taken into account by considering the final obtained shape. The method is completely tool-independent and is only based on the reference points-based surrogate model, depending on the nominal part. This allows the tools to be adapted on the basis of the effective contours and the same setup configuration to be maintained in every forming simulation.

Conclusions

The process of tool design in bulk metal forming is a time- and resource-consuming task, which is often tackled by trial-and-error and experience-based approaches. The equivalent surrogate model developed in this work enables a reduction in the effort required in compensating for the arising deviations and enhances the efficiency of the compensation process for axisymmetric parts. The surrogate model consists of a set of reference points, which are defined by the user by a radial and cross-section partitioning. On the basis of their deviations, the deformed shape is interpolated with B-splines, which allows to derive the nodal deviations for the compensation simulations. The compensation algorithm represents an enhancement of the DC-SF method and consists of two FE simulations. In the first step, the nominal geometry is deformed to the deviating shape and the resulting compatible stress field is recorded. Subsequently, the compatible stresses are applied to the nominal geometry and the compensated shape is obtained by relaxation. The updated tools are retrieved by substitution of the effective contours and through B-spline interpolation in parametric form. The compensation strategy is validated with a case-study geometry. Numerical results show that after four iterations the part tolerances lie in the class $IT8 \div 10$, while the experimental tests attain up to $IT10$. This represents a good improvement in the typical accuracy level in open-die forging. The robustness of the algorithm is demonstrated by analysing an additional nominal geometry, which shows faster convergence and a similar accuracy level. The proposed compensation method exhibits low computational time, requires only elastic analyses and can theoretically be applied to any forming process. In particular, the presented strategy can be beneficial for the design of components related to the automotive industry. Engine parts, such as connecting rods and clutch covers, as well as chassis units, such as control arms and joints, can be manufactured with reduced time and effort. Further investigations concern the extension of the presented strategy to one of the mentioned industrial applications, considering the efficiency gain of the implemented method with respect to the traditional ones. Moreover, additional studies may extend this strategy to unsymmetrical parts as well as to sheet metal forming, focusing on the representation of the deformed and updated shapes by B-splines and NURBS surfaces.

Funding The authors would like to thank the German Research Foundation (Deutsche Forschungsgemeinschaft, DFG) for financial support, provided under the grant numbers VO 1487/26 − 1. Open Access funding enabled and organized by Projekt DEAL.

Compliance with Ethical Standards

Conflict of interests The authors declare that they have no conflict of interest.

Appendix

Compensation results tabular data

Table 3 Tabular results data for the nominal geometry

Iteration	Upper die				Lower die			
	$\bar{u}$ $[mm]$	$\Delta u\%_{rel}$ $[-]$	$\Delta u\%_{abs}$ $[-]$	IT [-]	$\bar{u}$ $[mm]$	$\Delta u\%_{rel}$ $[-]$	$\Delta u\%_{abs}$ [-]	IT [-]
0	0.20	–	–	IT12	0.19	–	–	IT12
1	0.14	−31.9%	−31.9%	IT11	0.18	−6.3%	−6.3%	IT12
2	0.13	−3.1%	−34.0%	IT11	0.10	−40.1%	−43.9%	IT10
3	0.09	−32.9%	−55.8%	IT10	0.06	−42.2%	−67.6%	IT9
4	0.08	−13.6%	−61.8%	IT10	0.05	−05.5%	−69.4%	IT8
5	0.10	29.7%	−50.5%	IT10	0.05	−14.2%	−73.7%	IT8
6	0.11	3.9%	−48.5%	IT11	0.05	−2.5%	−74.4%	IT8
7	0.09	−15.2%	−56.3%	IT10	0.05	5.7%	−73.0%	IT8

Table 4 Tabular results data for the robustness analysis geometry

Iteration	Upper die				Lower die			
	$\bar{u}$ $[mm]$	$\Delta u\%_{rel}$ $[-]$	$\Delta u\%_{abs}$ $[-]$	IT [-]	$\bar{u}$ $[mm]$	$\Delta u\%_{rel}$ $[-]$	$\Delta u\%_{abs}$ [-]	IT [-]
0	0.16	–	–	IT12	0.21	–	–	IT12
1	0.09	−41.3%	−41.3%	IT10	0.04	−82.9%	%−82.9%	IT9
2	0.03	−66.3%	−80.2%	IT8	0.03	−27.1%	%−87.5%	IT8
3	0.06	104.3%	−59.6%	IT9	0.01	−71.5%	%−96.4%	IT4

Table 5 Tabular results data for the experimental geometry

Iteration	Upper die				Lower die			
	$\bar{u}$ $[mm]$	$\Delta u\%_{rel}$ $[-]$	$\Delta u\%_{abs}$ $[-]$	IT [-]	$\bar{u}$ $[mm]$	$\Delta u\%_{rel}$ $[-]$	$\Delta u\%_{abs}$ [-]	IT [-]
0	0.30 ± 0.02	–	–	IT13	0.53 ± 0.07	–	–	IT14
1	0.12 ± 0.01	$-18.1\% \pm 3.0\%$	$-60.6\% \pm 14.4\%$	IT10	0.34 ± 0.03	$-19.4\% \pm 9.7\%$	$-36.1\% \pm 22.7\%$	IT13

Compensation results on single reference points, nominal geometry

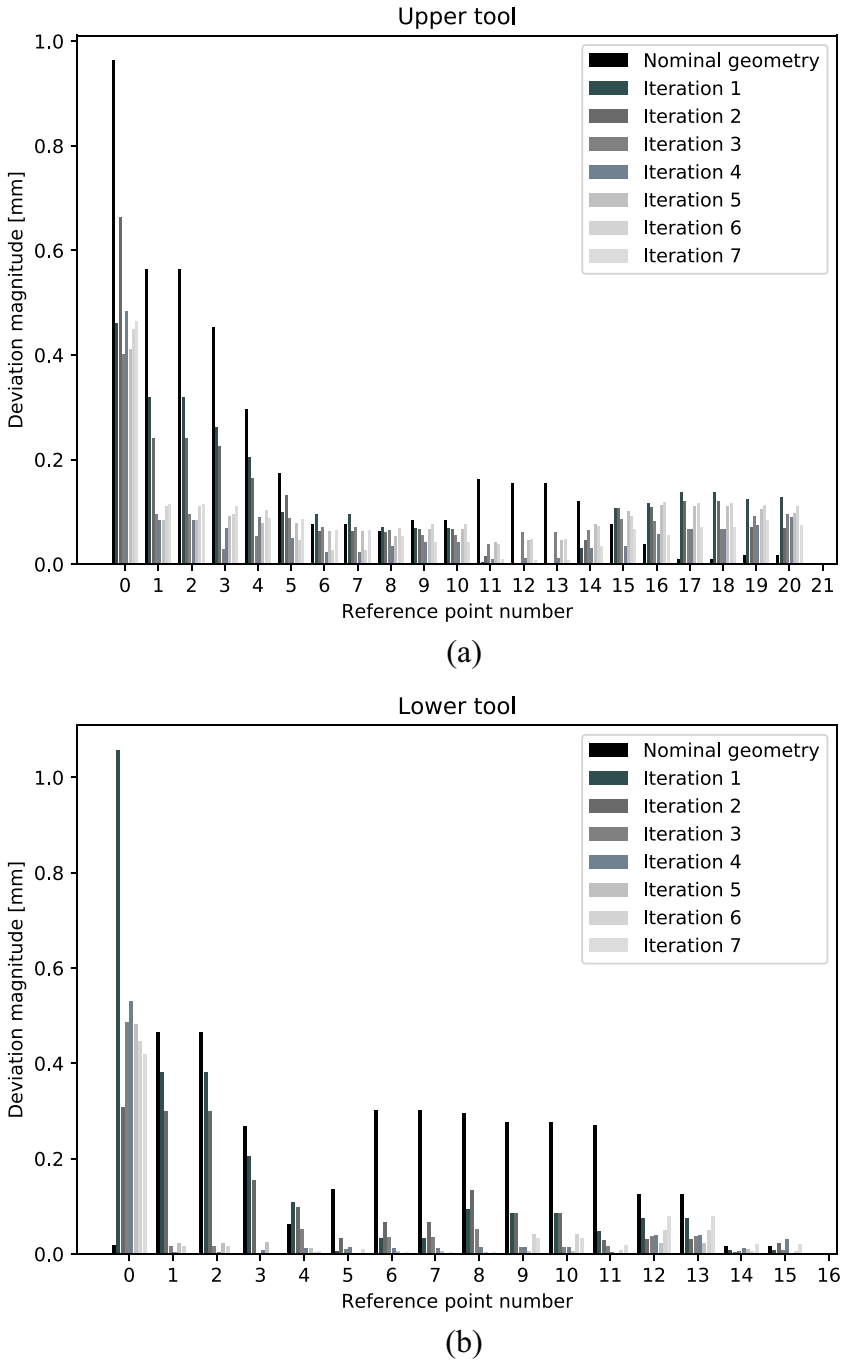

Fig. 13 Magnitude of deviation $\bar{u}_{mag}$ on single reference points for the virtual compensation: **a** case-study geometry, upper contour; **b** case-study geometry, lower contour

References

1. Behrens B-A, Odening D (2009) Process and tool design for precision forging of geared components. Int J Mater Form 2(SUPPL. 1):125–128. https://doi.org/10.1007/s12289-009-0577-7. https://www.scopus.com/inward/record.uri?eid=2-s2.0-84856033223&doi=10.10072fs12289-009-0577-7&partnerID=40&md5=319ba51346d09d531833ce4bcd77dc5e
2. Balendra R (2001) Nett-shape forming: state-of-the-art. J Mater Process Tech 115(2):172–179. https://doi.org/10.1016/S0924-0136(01)00812-3
3. Geng L, Wagoner RH (2002) Role of plastic anisotropy and its evolution on springback. Int J Mech Sci 44(1):123–148. https://doi.org/10.1016/S0020-7403(01)00085-6
4. Maier D, Hartmann C, Till M, Büdenbender C, Behrens B-A, Volk W (2019) Data-driven compensation for bulk formed parts based on material point tracking. Key Eng Mat 794:277–284. https://doi.org/10.4028/www.scientific.net/KEM.794.277
5. Lee S, Eder M, Maier D, Volk W (2019) Stress-based compensation of geometrical deviations in metal forming. In: Schmitt R, Schuh G (eds) Advances in production research, vol 203, pp 647–656. Springer International Publishing. Cham
6. Hartmann C, Eder M, Opritescu D, Maier D, Santaella M, Volk W (2018) Geometrical compensation of deterministic deviations for part finishing in bulk forming. J Mater Process Tech 261:140–148. https://doi.org/10.1016/j.jmatprotec.2018.06.008
7. Li KP, Carden WP, Wagoner RH (2002) Simulation of springback. Int J Mech Sci 44(1):103–122. https://doi.org/10.1016/S0020-7403(01)00083-2
8. Carden WD, Geng LM, Matlock DK, Wagoner RH (2002) Measurement of springback. Int J Mech Sci 44(1):79–101. https://doi.org/10.1016/S0020-7403(01)00082-0
9. Karafillis AP, Boyce MC (1992) Tooling design accomodating springback errors. J Mater Process Tech 32(1-2):499–508. https://doi.org/10.1016/0924-0136(92)90206-8
10. Karafillis AP, Boyce MC (1992) Tooling design in sheet metal forming using springback calculations. Int J Mech Sci 34(2):113–131. https://doi.org/10.1016/0020-7403(92)90077-T
11. Karafillis AP, Boyce MC (1996) Tooling and binder design for sheet metal forming processes compensating springback error. J Phys Conf Ser 36(4):503–526. https://doi.org/10.1016/0890-6955(95)00023-2
12. Wu L (1997) Tooling mesh generation technique for iterative FEM die surface design algorithm to compensate for springback in sheetmetal stamping. Eng Computations 14(6):630–648. https://doi.org/10.1108/02644409710180491
13. Wu L (1996) Generate tooling mesh by FEM virtual forming model for springback compensation in die surface design of sheet metal stamping. SAE Trans 105:643–649
14. Gan W, Wagoner RH (2004) Die design method for sheet springback. Int J Mech Sci 46(7):1097–1113. https://doi.org/10.1016/j.ijmecsci.2004.06.006
15. Lingbeek RA, Gan W, Wagoner RH, Meinders T, Weiher J (2008) Theoretical verification of the displacement adjustment and springforward algorithms for springback compensation. Int J Mater Form 1(3):159–168. https://doi.org/10.1007/s12289-008-0369-5
16. Birkert A, Hartmann B, Straub M (2017) New method for springback compensation for the stamping of sheet metal components. J Phys Conf Ser 896:012067. https://doi.org/10.1088/1742-6596/896/1/012067
17. Hiramoto J, Urabe M, Ishiwatari A, Yoshida F (2016) Simple springback cause analysis using measured shapes of dies and pressed part. Key Eng Mat 725:683–688. https://doi.org/10.4028/www.scientific.net/KEM.725.683
18. Fourment L, Chenot JL (1996) Optimal design for non-steady-state metal forming processes—i. shape optimization method. Int J Numer Methods Eng 39(1):33–50. https://doi.org/10.1002/(SICI)1097-0207(19960115)39:1<33::AID-NME844>3.0.CO;2-Z, https://onlinelibrary.wiley.com/doi/abs/10.1002/%28SICI%291097-0207%281%9960115%2939%3A1%3C33%3A%3AAID-NME844%3E3.0.CO%3B2-Z
19. Vieilledent D, Fourment L (2001) Shape optimization of axisymmetric preform tools in forging using a direct differentiation method. Int J Numer Methods Eng 52(11):1301–1321. https://doi.org/10.1002/nme.256
20. Rodič T, Grešovnik I (1998) A computer system for solving inverse and optimization problems. Eng Comput 15:893–907. https://doi.org/10.1108/02644409810236902
21. Ghouati O, Lenoir H, Gelin JC (2000) Optimal design of forming processes using the finite element method. Adv Eng Mater 2(7):438–442. https://doi.org/10.1002/1527-2648(200007)2:7<438::AID-ADEM438>3.0.CO;2-I, https://onlinelibrary.wiley.com/doi/abs/10.1002/1527-2648%28200007%292%3A7%3C438%3A%3AAID-ADEM438%3E3.0.CO%3B2-I
22. Ou H, Armstrong CG (2002) Die shape compensation in hot forging of titanium aerofoil sections. J Mater Process Tech 125-126:347–352. https://doi.org/10.1016/S0924-0136(02)00297-2
23. Lu B, Ou H, Armstrong CG, Rennie A (2009) 3d die shape optimisation for net-shape forging of aerofoil blades. Materials & Design 30(7):2490–2500. https://doi.org/10.1016/j.matdes.2008.10.007
24. Landkammer P (2018) Inverse fomfindungsverfahren zur anwendung in der umformtechnik. Ph.D. Thesis, Friedrich-Alexander-Universität Erlangen-Nürnberg
25. Landkammer P, Caspari M, Steinmann P (2018) Improvements on a non-invasive, parameter-free approach to inverse form finding. Comput Mech 61(4):433–447. https://doi.org/10.1007/s00466-017-1468-2
26. Caspari M, Landkammer P, Steinmann P (2018) A non-invasive node-based form finding approach with discretization-independent target configuration. Advanced Modeling and Simulation in Engineering Sciences 5(1):725. https://doi.org/10.1186/s40323-018-0104-9
27. Hartmann C, Eder M, Opritescu D, Volk W (2017) Process-integrated compensation of geometrical deviations for bulk forming. Procedia Eng 207:466–471. https://doi.org/10.1016/j.proeng.2017.10.806
28. Hartmann C, Opritescu D, Volk W (2019) An artificial neural network approach for tool path generation in incremental sheet metal free-forming. J Intell Manuf 30(2):757–770. https://doi.org/10.1007/s10845-016-1279-x
29. Zienkiewicz OC, Zhu JZ, Taylor RL (2013) The finite element method: Its basis and fundamentals, 7th edn. Butterworth-Heinemann, Oxford, UK

30. Dassault Systemes (2013) Abaqus 6.13 documentation. Dassault Systemes, Vélizy-Villacoublay. http://dsk.ippt.pan.pl/docs/abaqus/v6.13/index.html
31. van Rossum G, Drake FL (2009) Python 3 reference manual. CreateSpace, Scotts Valley, CA. https://www.python.org/
32. Piegl L, Tiller W (1997) The nurbs book. Monographs in visual communication, 2nd edn. Springer, Berlin and Heidelberg. https://doi.org/10.1007/978-3-642-59223-2
33. Bingol OR, Krishnamurthy A (2019) Nurbs-python: An open-source object-oriented nurbs modeling framework in python. SoftwareX 9:85–94. https://doi.org/10.1016/j.softx.2018.12.005
34. Dassault Systemes (2009) Catia v5 documentation. Dassault Systemes, Vélizy-Villacoublay. http://catiadoc.free.fr/online/CATIA_P3_default.htm
35. Behrens B-A, Volk W, Maier D, Scandola L, Ott M, Büdenbender C, Till M (2020) A combined numerical and experimental investigation on deterministic deviations in hot forging processes. Procedia Manufacturing 47:295–300. https://doi.org/10.1016/j.promfg.2020.04.231. 23rd International Conference on Material Forming
36. Herbertz R (2013) Massivumformung kurz und bündig, 1Aufl. Industrieverband Massivumformung e.V, Hagen